

Total Electron Content Prediction Model using the Artificial Neural Networks over the Eastern Africa Region

Emmanuel D Sulungu^{1*} and Christian BS Uiso²

¹*Department of Physics, The University of Dodoma, Tanzania*

**Corresponding author e-mail: edsulungu@gmail.com*

²*Marian University College, Bagamoyo, Tanzania*

E-mail: cbsuiso2010@gmail.com

Abstract

In this paper, development of a model using NN technique for prediction of GPS TEC over the Eastern Africa region is presented. TEC data was obtained from the Africa array and IGS network of ground based dual-frequency GPS receivers from 18 stations within the East African region. It covers approximately the area from ~2.6°N to ~26.9°S in magnetic latitudes and from ~95°E to ~112°E in magnetic longitudes. The input layer of the developed model consisted of seven neurons which were selected by considering the parameters that are known to affect the TECv data. The results showed that when the number of hidden layer neurons surpassed about 18, the RMSEs were noted to continuously increase indicating poor predictions beyond this number. The RMSE at this point was observed to be about 5.2 TECU which was lowest of all. The errors and relative errors were fairly small. Developed NN model estimated GPS TECv very well compared to IRI model. It is established in this study that, the IRI electron density at F2 peak (NmF2) gives good GPS TECv prediction when added as an input neuron to the NN.

Keywords: GPS, GPS TECv, Total Electron Content, Neural Network

Introduction

Global Positioning System (GPS) has been widely used in scientific studies to develop an improved understanding of the ionosphere and plasmasphere. It is used to provide users with navigation, positioning and time information on a global scale (Norsuzila et al. 2010). However, the GPS has become widespread for providing information about the total electron content (TEC) within the ionosphere (Liu et al. 2013). TEC is important in providing the ionospheric description in general and has many practical applications, for example; satellite navigation, time delay and range error corrections for single frequency GPS satellite signal receivers (Bhuyan and Borah 2007).

GPS receivers are not installed at every location on the earth to allow global measurements of TEC. This has led to the importance of having some models that will help to get data from the locations with no data

to understand the global behavior of the TEC. In this study we aimed at developing a model for predicting GPS derived TEC using Neural Networks (NNs).

NNs are the powerful tools for predictive modeling with the ability of machine learning as well as pattern recognition. They can learn trends and patterns in specific data given to them and therefore be able to predict correctly future trends and patterns for the data. It has also been shown that a neural network can be trained to perform a particular function by adjusting the weights (Demuth and Beale 2002, Okoh et al. 2016). The strength of neural networks is based on the fact that, they have the ability to represent both linear and nonlinear relationships directly from the data being modeled (Okoh et al. 2016).

A number of studies carried out at different locations have demonstrated the capability of neural networks in ionospheric modeling. Okoh

et al. (2016) in their study on a regional GNSS-VTEC model over Nigeria using neural networks, observed that disturbance storm time (DST), sunspot number (SSN), and IRI-foF2 as input layer neurons on the networks are effective in increasing the network performances. A study by Habarulema et al. (2007) on prediction of global positioning system total electron content showed that, neural networks are suitable for predicting the GPS TEC values at locations within South Africa and also their results were able to predict the TEC values more accurately than IRI-2001. They further showed that, the NN model accurately predicted the trend of GPS TEC diurnally and seasonally, although in some instances, the developed model overestimated or underestimated the TEC. The observation by Homam (2014) revealed that, a network configuration which utilized TEC values during lower solar activity gives a better root mean square error (RMSE), and both absolute and relative error, in comparison with the configurations which used TEC values during relatively higher solar activity. Another study on a neural network approach for regional vertical total electron content modeling was conducted by Leandro and Santos (2007) using Brazilian network. The results showed that, neural network model provided estimates of TEC_v values with an average absolute error of 3.7 TECU with standard deviation of 2.7 TECU.

Tulunay et al. (2004) introduced the Middle East Technical University Neural Networks model to forecast 10 min TEC variations during high solar activity of the years 2000–2001 and obtained a satisfactory sensitivity and accuracy of NN model. They concluded that,

the methods that they developed can be used for characterizing the electromagnetic wave propagation medium for the purposes of radio system planning and operation. In their studies on TEC prediction with neural network at equatorial latitude station in Thailand, Watthanasangmechai et al. (2012) observed a good prediction of TEC by NN model compared with the IRI-2007 model. Their results further revealed a considerable difficulty for the NN to learn during some periods due to large variations of TEC, and associated this difficulty with the occurrence of an equatorial plasma bubble and with day-to-day TEC variations in the equatorial region. The work by Uwamahoro and Habarulema (2015) when they were modeling total electron content during geomagnetic storm conditions in South Africa suggests the selection of hidden node number as the reason that could affect the NN prediction capability.

In the present study we focus on developing a model using neural network technique for significant prediction of GPS TEC over the Eastern Africa region.

Materials and Methods

TEC data were obtained from the Africa array and IGS network of ground based dual-frequency GPS receivers within the East African region as shown in Figure 1. The network array comprised of 18 stations (Table 1) covers approximately the area from 17°S to 12°N in geographical latitude (magnetic lat. ~2.6°N to ~26.9°S) and from 26°E to 40°E in geographical longitude (magnetic long. ~95°E to ~112°E). The data from these stations were obtained from the UNAVCO website (<http://www.unavco.org/>).

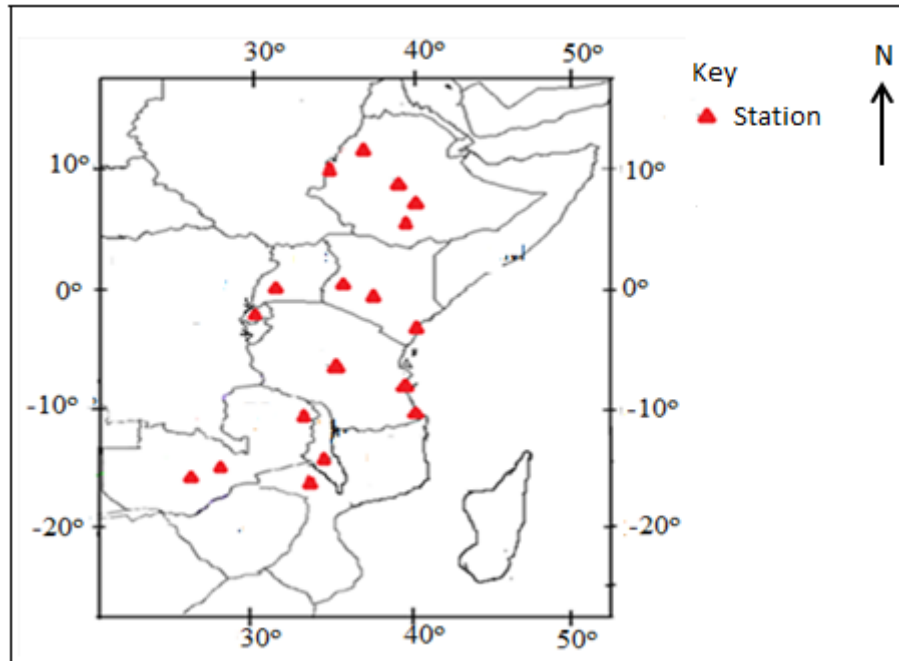


Figure 1: Eastern Africa map showing the network of GPS receivers used to derive TEC for NN model development.

Table 1: GPS receiver stations with their corresponding latitudes and longitudes

Country	Station		Geographic		Geomagnetic	
	Name	Code	Latitude	Longitude	Latitude	Longitude
Tanzania	Dodoma	DODM	6.19°S	35.75°E	16.10°S	107.22°E
	Mtwara	MTVE	10.26°S	40.17°E	20.35°S	111.25°E
	Tanz. CGPS	TANZ	6.77°S	39.21°E	16.59°S	110.65°E
Kenya	Malindi	MAL2	2.99°S	40.19°E	12.42°S	111.86°E
	Eldoret	MOIU	0.29°N	35.29°E	9.17°S	107.00°E
	Nairobi	RCMN	1.22°S	36.89°E	10.69°S	108.59°E
Uganda	Mbarara	MBAR	0.60°S	30.74°E	10.22°S	102.36°E
Ethiopia	Asosa	ASOS	10.06°N	34.55°E	0.70°N	106.17°E
	Bahir Dar	BDAR	11.60°N	37.36°E	2.64°N	108.98°E
	Robe	ROBE	7.11°N	40.03°E	1.69°S	111.78°E
	Nazret	NAZR	8.57°N	39.29°E	0.25°S	111.01°E
	Negele	NEGE	5.34°N	39.59°E	3.59°S	111.36°E
Rwanda	Kigali	NURK	1.95°S	30.09°E	11.63°S	101.66°E
Malawi	Zomba	ZOMB	15.38°S	35.33°E	26.07°S	105.58°E
Mozambique	Tete	TETE	16.15°S	33.58°E	26.94°S	103.66°E
Zambia	Mzuzu	MZUZ	11.43°S	34.01°E	21.88°S	104.92°E
	Itezi-Tezi	TEZI	15.75°S	26.02°E	26.59°S	95.95°E
	Lusaka	ZAMB	15.43°S	28.31°E	26.27°S	98.40°E

GPS data were processed into TEC data using the GPS-TEC processing software developed by Gopi Krishna Seemala (<http://seemala.blogspot.com/>). This software allows for the extraction of TECv from the GPS measurements. It reads raw data, processes cycle slips in phase data, reads satellite biases from International GNSS Service (IGS) code file (if not available, it calculates them), calculates receiver bias, and calculates the interchannel biases for different satellites in the receiver. It calculates the slant TEC (TECs) along the path of the GPS signal using equation

$$TECs = \frac{1}{40.3} \left(\frac{f_1^2 f_2^2}{f_1^2 - f_2^2} \right) (P_1 - P_2) \quad (1)$$

where P_1 and P_2 are pseudoranges observable on L1 and L2 signals, f_1 and f_2 are the corresponding high and low GPS frequency, respectively. Then, TECs measured at an interval of 30 s were converted to TECv using the mapping function $M(e)$, which takes the curvature of the Earth into account (Shim 2009) as follows:

$$TECv = M(e) \times TECs - (b_s + b_r + b_{rx}) \quad (2)$$

where b_s is satellite bias, b_r is a receiver bias and b_{rx} is a receiver interchannel bias, and

$$M(e) = \left[1 - \left(\frac{\cos(e)}{1 + h/R_E} \right)^2 \right]^{\frac{1}{2}} \quad (3)$$

Here e is an elevation angle of a satellite, h is ionospheric shell height assumed to be 350 km in this study, and R_E is the Earth's mean radius. To ensure the data used have no undesirable errors which might result from the effect of multipath, a minimum elevation angle of 30° was used.

The input layer of the developed model based on neural network consisted of seven neurons which were selected by considering the parameters that are known to affect the TECv data such as the year, day of the year,

hour of the day, latitudes, longitudes, the sunspot number (SSN) and the IRI electron density at F2 peak (NmF2). The first three inputs help the network in learning temporal variations. The year represents solar cycle variations, the day of the year represents seasonal variation and the hour of the day represents diurnal variation. The fourth and fifth inputs represent the spatial variations and the sixth is used as a measure of solar activity. SSN were obtained from the WDC-SILSO website, <http://www.sidc.be/silso/datafiles>.

The seventh input is used to aid the learning in TECv variations because both TECv and NmF2 normally demonstrate identical day-to-day variations (Leitinger et al. 2004, Jin and Maruyama 2009), and this is a new approach as established in this study. The IRI-NmF2 values have been chosen rather than measured values because of scarce instruments for measuring this parameter within the region in study. However, using IRI-NmF2 values facilitates predictions of TECv at all anticipated locations and time periods within the eastern part of the African sector. Furthermore, the use of NmF2 from IRI was considered since the IRI is an empirical model established using accessible data from all around the world, and has been widely accepted as a reliable ionospheric model that has incorporated long-term solar cycle variation (Okoh et al. 2016). Hence, supports the networks' capacity to learn long-term variations especially for regions with short period data. For effective learning of input-target links, an 11-year dataset is required as the results of the solar cycle variations. Thus the insertion of the IRI model as an additional input neuron improves the networks in learning solar cycle variations.

In this study, the multi-layer perceptron neural network was used because of its speed and effectiveness during learning process (Okoh et al. 2016, Razin et al. 2015). Also, one input layer, one hidden layer and one output layer were used (Figure 2).

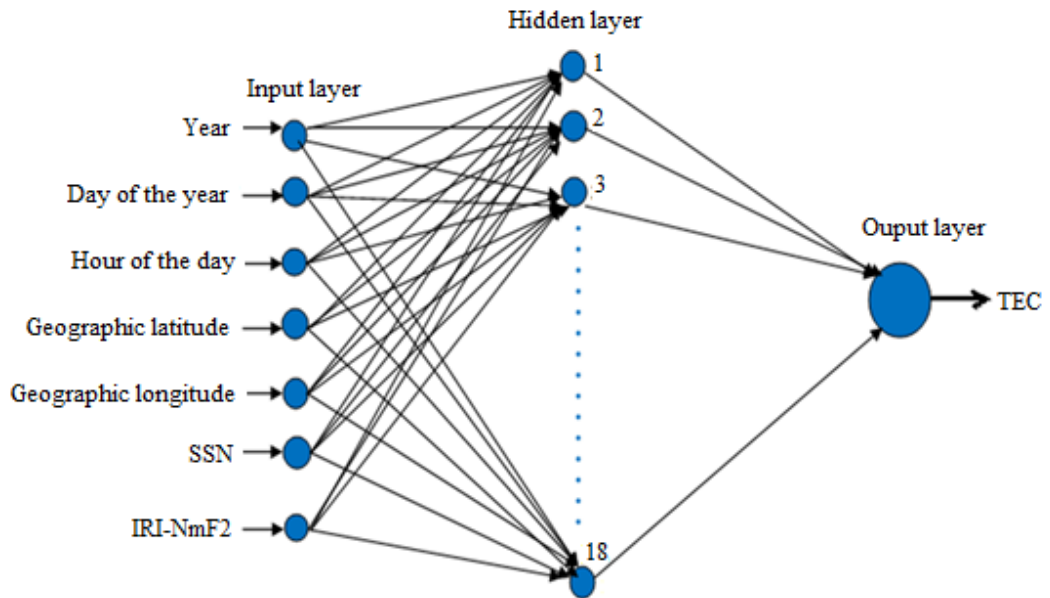


Figure 2: Schematic diagram showing the neural network used in this study.

In order to obtain the optimal number of neurons in the hidden layer, four different networks configurations were trained varying depending on the number and type of input neurons used as follows:

- (i) The first network consisted of five neurons; year, day of the year, hour of the day, geographic latitudes and geographic longitudes.
- (ii) The second network comprised of six neurons; all input neurons used in the first network and SSN as an additional input neuron.
- (iii) The third network comprised of six neurons also; all input neurons used in the first network and IRI-NmF2 as an additional input neuron.
- (iv) The fourth network comprised of seven input neurons; year, day of the year, hour of the day, geographic latitudes, geographic longitudes, SSN and IRI-NmF2.

Each of the four systems of networks used to train the neural network was simulated 50 times by varying the number of the hidden layer neurons from 1 to 50. The RMSE was

used to choose the number of hidden layer neurons which performs better than others. Among the four systems trained, decision of the best network was done based on the most minimum RMSE on various configurations. The RMSE method has been commonly used as a means to decide optimal factors for statistically based predictions such as solar and geomagnetic activity data predictions, solar cycle predictions using neural networks and modeling of the interaction between solar wind and magnetosphere (Conway et al. 1998, Habarulema 2010).

The dataset used in this study was from the quietest day of each month for the period of 2012-2016. The TECv values averaged hourly were used as the output of the neural network for the specified period. From the available dataset within the period 2012 -2015, 70% of it was used in training the neural network, 15% for validation and the remaining 15% for random testing. Dataset from Mbarara (0.6°S, 30.74°E) for 2016 were used in testing and these were randomly chosen. The decision of using data from Mbarara were purposely for testing the temporal performance of the model

since these data are from outside the period of the data used in training, validation and random testing.

Likewise, in order to test the performance of the neural network model at different times, the results were compared by the TEC_v values of the test station. Different times in a day selected for testing were 3:00 UT (6:00 LT), 9:00UT (12:00 LT) and 15:00 UT (18:00 LT). These times of the day were chosen in order to test the model near the time of sunrise (6:00 LT), a time when production of the solar EUV starts, during noon (12:00 LT), a time of the day with higher ionospheric activities and near the time of sunset (18:00 LT), a time when production of the solar EUV ceases. On the other hand, the results of the neural network model were also tested at different seasons of the year; March equinox, June solstice, September equinox and December solstice. Using these procedures, the performance of the model for predictions within the area covered by the network of GPS receivers was investigated.

In order to evaluate the capability of the performance of the model, the prediction errors (absolute errors) and the relative errors of the models were computed using the following equations:

$$|e| = |TEC_{NN} - TEC_{GPS}| \quad (4)$$

$$|\varepsilon| = \frac{|e|}{TEC_{GPS}} \times 100 \quad (5)$$

Where: $|e|$ = prediction (absolute) error, $|\varepsilon|$ = relative error, TEC_{NN} = TEC estimated by the NN model, TEC_{GPS} = measured TEC obtained from the GPS receivers.

Results and Discussion

In this section, the results of the four trained neural network architectures for GPS TEC_v prediction are presented so as to select the one that provides the optimal results. The RMSEs of the neural network (NN) TEC_v from GPS

TEC_v and correlations coefficients between the GPS TEC_v and the NN TEC_v are also presented. Finally, comparison of hourly and seasonal values of the NN modeled TEC_v with GPS TEC_v is conferred.

Statistical analysis of GPS-TEC and NN-TEC

Figures 3 and 4 show the RMSEs for random dataset and Mbarara station (16.15°S, 33.58°E) dataset, respectively, while Figure 5 shows scatter plots of GPS TEC_v versus TEC_v obtained from the NN model over Mbarara station.

From the figures, it is clearly seen that network 4 presented the best results since its RMSEs were lower than those from the other three networks, indicating good agreements between the measured values and the network estimated values when the NmF2 is added as an input neuron. However, from Figure 3, it was observed that, the 15% random test data displayed a continuous general decrease of the RMSEs with the increase in the number of hidden layer neurons. Okoh (2016) suggested that, if the test data used is randomly picked, it is very possible for RMSEs to continuously decrease when the number of hidden layer neurons increases. This scenario occurs when data used for testing are within the range of data used for the training.

Figure 4 which presents the results for test station clearly provided the optimal results for NN configurations used in testing. From the figure, it was observed that, when the number of hidden layer neurons surpassed about 18, the RMSEs were noted to continuously increase indicating poor predictions beyond this number. This scenario occurred because when the number of hidden layers goes above 18, the networks are said to be over-trained (Okoh 2016). The RMSE at this point were observed to be about 5.2 TECU which was lowest of all.

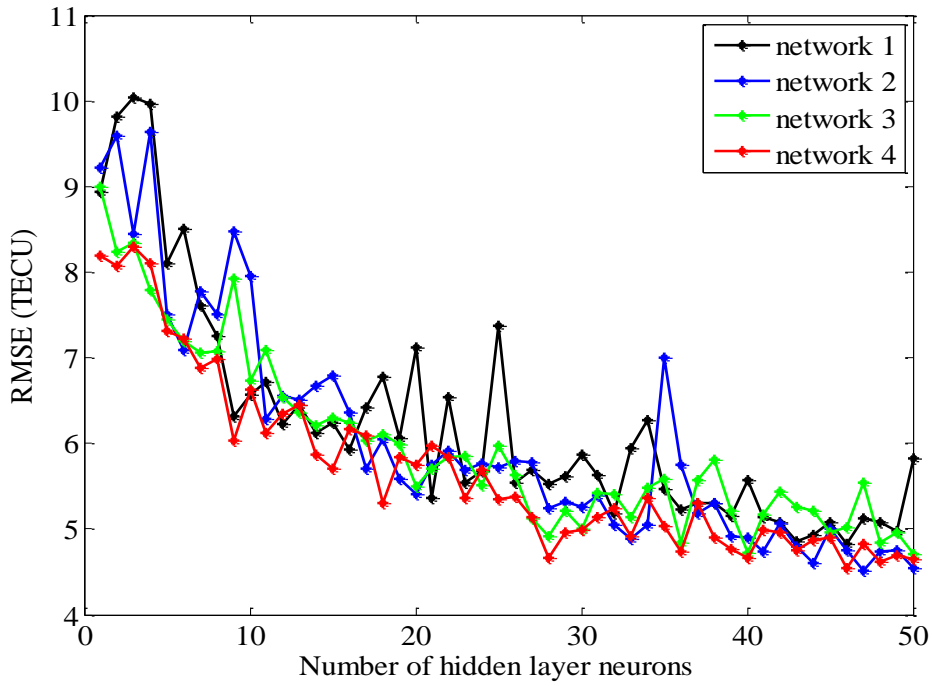


Figure 3: A plot of RMSEs using random dataset for all the four networks.

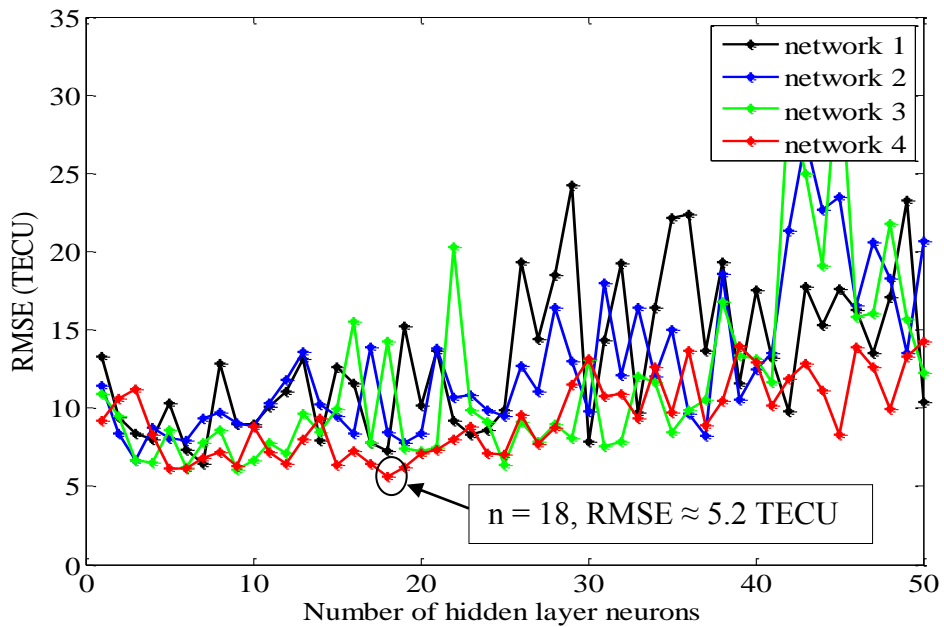


Figure 4: A plot of RMSEs using Mbarara station dataset for all the four networks.

On the other hand, network 1 presented the poorest results with higher RMSEs. This scenario is due to the fact that, the learning capacity of neural networks is facilitated by the increase in number of the neurons in the input layer. Networks 2 and 3 provided better results as compared to network1, but not as good as network 4. It is thus established that, the more input layer neurons are additionally included to the network, the better the networks learn and give the best results.

Figure 5 presents the scatter plots for targets (GPS TECv) versus outputs (TECv obtained from the NN prediction model) over the test station; Mbarara station from January

to October 2016, with lines of best fit inserted to the plot, as well as the correlation coefficients. From the figure, it is observed that correlation coefficients provided good levels of reliability of the developed NN model to estimate GPS TECv.

From the same figure, it is clearly seen that, GPS TECv was highly correlated to NN TECv. The highest correlation coefficient (r) was 0.9770 obtained during August and lowest correlation coefficient (r) was 0.9118 obtained during July. These correlation coefficients indicated better agreement in trend between the predictions and the observations when the IRI-NmF2 was included as an input layer neuron.

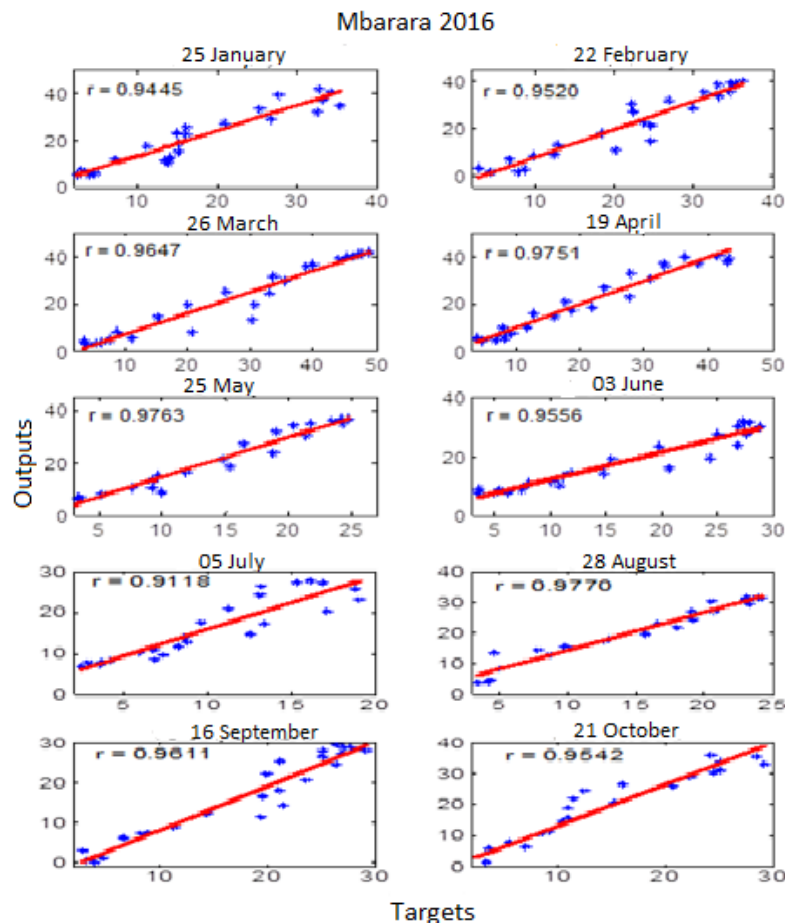


Figure 5: A plot of Outputs versus Targets for Mbarara during January - October 2016.

Comparison of hourly values of the NN modeled TEC_v with GPS TEC_v

To assess the effectiveness of NN output in predicting GPS TEC_v at some periods within a day, NN results were compared with GPS TEC_v from selected times of the day using data from Mbarara (2016) as a test station from January to October. There was no data for the specified year during November and December, which might be due to instrumental failures and electrical power shutdowns. Different times in a day selected for testing were 3:00 UT (6:00 LT), 9:00 UT (12:00 LT), 15:00 UT (18:00 LT) and 21:00 UT (0:00 LT). The difference between universal time and the local time in the study region is three hours. Thus the selection of these times was based on different sun activities in a day such as midnight, sunrise, noon and sunset.

Figure 6 illustrates the hourly comparison of the NN model TEC_v values with the TEC_v obtained from GPS receivers over Mbarara station in 2016. From the figure, it is clearly shown that, NN model results closely matched with the GPS TEC_v values in most of the times for the specified period. Figures 7 and 8 show the errors of NN model predictions from GPS TEC_v and their corresponding relative errors, respectively. The errors and relative errors were fairly small which indicated good prediction of GPS TEC_v by the NN model over the eastern part of the African sector represented by Mbarara as a test station.

At 3:00 UT (6:00 LT), (left upper panel of Figure 6), it is observed that, NN model and GPS TEC_v closely matched giving a correlation coefficient of 0.9277 (Table 2) which was very good. In February, September and October, the errors were above 2.5 TECU but less than 4 TECU. But, in the rest of the months the errors were below 1 TECU (Figure 7) which indicated a good prediction of the developed model. The maximum relative error of NN model to the GPS TEC_v was observed to be about 52% occurred in October while the minimum was about 0.3% occurred in January (Figure 8).

Comparison of NN model with GPS TEC_v at 9:00 UT (12:00 LT) over Mbarara station in the year 2016 is shown in the right upper panel of Figure 6. From the figure, a fairly good agreement was observed between NN model and the TEC_v obtained from GPS receiver having a correlation coefficient of 0.7327 as presented in Table 2. Although this correlation coefficient was not as good as that at 3:00 UT (12:00 LT), but the errors and relative errors were significantly small indicating a good prediction of GPS TEC_v by the NN model at this particular hour. The maximum error of NN model prediction from GPS TEC_v was about 7 TECU occurred in May and the minimum was about 0.3 TECU observed in April (Figure 7). On the other hand, the maximum and minimum relative errors of NN model to the GPS TEC_v as shown in Figure 8 were about 21% and 1%, respectively which were fairly small indicating a good prediction by the model.

At 15:00 UT (18:00 LT), (left lower panel of Figure 6), NN model matched with the GPS TEC_v with a correlation coefficient of 0.8861 (Table 2) which was reasonably good. The maximum error occurred from the prediction of GPS TEC_v by the NN model at this hour was about 7.6 TECU observed during August while the minimum was 0.1 TECU observed during June (Figure 7). Correspondingly, the maximum and minimum relative errors observed at this particular hour of the day were approximately 16% and 0.2%, respectively (Figure 8). These were fairly small errors for predictions by the model which indicated a good agreement between the modeled TEC_v and the observed TEC_v.

Comparison between the NN modeled TEC_v and the GPS derived TEC_v at 21:00 UT (0:00 LT) over Mbarara station in 2016 is presented in Figure 6 (right lower panel). The figure depicts good prediction of GPS TEC_v by the NN model although the correlation coefficient between these two quantities was small, i.e., $r = 0.3800$ (Table 2). The small correlation coefficient indicated unmatched trend between the two compared quantities, but the efficiency in prediction can also be

indicated by the errors and/or relative errors of one quantity to the other. Therefore, from Figures 7 and 8, the maximum and minimum errors of NN modeled TECv from GPS measured TECv were observed to be about 5 TECU observed during August and 0.2 TECU observed during January, respectively. Similarly, the corresponding maximum relative

error was about 29% and the minimum was about 1%. Hence, in spite of the small correlation coefficient between NN modeled TECv and the GPS measured TECv, the NN model predicted well the GPS TECv at 21:00 UT (0:00 LT) based on the errors and relative errors.

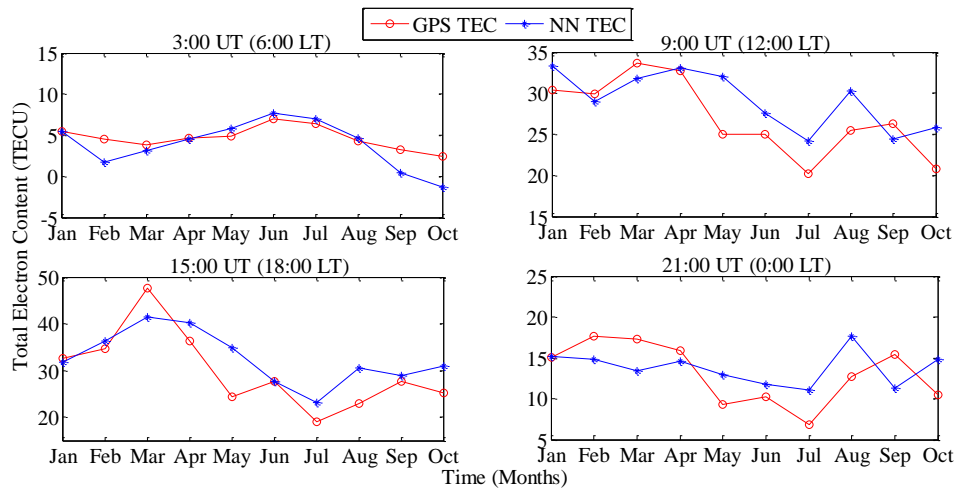


Figure 6: A plot of hourly comparison of GPS TECv and NN TECv for Mbarara 2016.

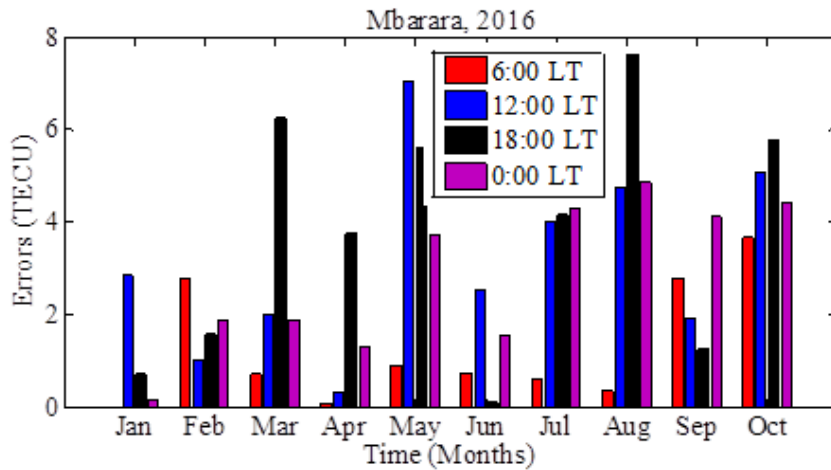


Figure 7: Plot of errors of NN TECv from GPS TECv for hourly comparison for Mbarara 2016.

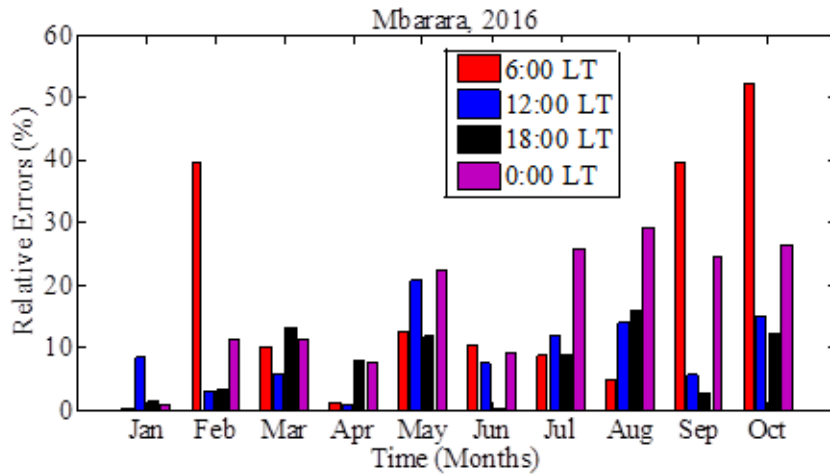


Figure 8: Plot of relative errors of NN TECv from GPS TECv for hourly comparison for Mbarara 2016.

Table 2: Hourly correlation coefficients for Mbarara 2016

Time	21:00 UT (0:00 LT)	3:00 UT (6:00 LT)	9:00 UT (12:00 LT)	15:00 UT (18:00 LT)
Correlation coefficient	0.38	0.9277	0.7327	0.8861

Comparison of seasonal values of the NN modeled TECv with the GPS TECv

It is well known that, seasons of the year have a significant contribution in TECv variation (Watthanasangmechai et al. 2012). Thus it was important to also perform a seasonal TECv comparison to investigate the capability of the developed NN model in predicting the GPS TECv during different seasons of the year. In order to accomplish this, three seasons of the year were identified, and one day (quiet day) in each season was selected and analysed as shown in Figures 9 and 10. The seasons were March equinox, June solstice and September equinox. Due to lack of data during December solstice, this season was excluded in the analysis. In this analysis, TECv from IRI 2012 model using NeQuick option for the topside Ne were also included. This was done in order to investigate the performance of the developed NN model comparing with an International model (IRI model) in predicting GPS TECv.

Seasonal comparison of GPS derived TECv with the TECv from NN model and IRI-2012 model for Mbarara station in 2016 is shown in Figure 9. The errors of predicted TECv by both NN model and IRI model from GPS measured TECv are presented in Figure 10, and Figure 11 presents their corresponding relative errors. The general observation showed that, NN model gave better estimates of the GPS TECv than the IRI model during all seasons for the specified year. It was also observed that, NN model well agreed with the GPS TECv during March equinox and June solstice, than it did during September equinox.

During March equinox (Figure 9, left upper panel), both NN model and IRI model closely matched the GPS TECv from 1:00 UT to 7:00 UT, and NN continued to well agree with GPS TECv up to 10:00 UT. During afternoon hours up to 24:00 UT, both models underestimated the GPS TECv, but NN model performed better than IRI model. The correlation coefficients between the GPS TECv and the TECv estimated by the NN model and IRI model

were equal to 0.9647 and 0.8361, respectively as presented in Table 3. On the other hand, from Figure 10 which displays the errors of NN TECv and IRI TECv from GPS TECv, it was found that, the maximum error of NN model TECv from GPS TECv was about 17 TECU observed at 21:00 UT, and the minimum error was about 0.05 TECU occurred at 5:00 UT. For the IRI model, the maximum and minimum errors were found to be 29.7 TECU and 0.22 TECU observed at 14:00 UT and 3:00 UT, respectively. Correspondingly, the maximum relative errors of NN model and IRI model were approximately 34.5% and 61%, respectively, while their minimum relative errors were about 0.08% and 0.45%, respectively (Figure 11). Based on this information, NN model showed reasonable performance in estimating the GPS TECv compared to IRI model, with a difference of more than 26% in their maximum relative errors.

Figure 9 (right upper panel) presents the results for comparison of GPS TECv with the TECv estimated by NN model and IRI model during June solstice. The observation from this month showed that, NN model closely agreed with GPS TECv throughout the day, with a correlation coefficient of 0.9556 as shown in Table 3. From the same figure it is clearly observed that, IRI model performed better in predicting GPS TECv during night hours than it did during the day, having a correlation coefficient of 0.8428. The performance of the two models was also compared using the errors they made in predicting GPS TECv and their corresponding relative errors as well. From Figure 10, the maximum error of NN model from GPS TECv was found to be approximately 5 TECU occurred at 1:00 UT, and the minimum was about 0.1 TECU occurred at 15:00 UT. For IRI model, the

maximum and minimum errors were about 11 TECU occurred at 12:00 UT and 1.5 TECU occurred at 1:00 UT, respectively. Likewise, the corresponding maximum relative errors of NN model TECv and IRI model TECv to the GPS TECv were observed to be about 18% and 39% respectively, and the minimum relative errors were about 0.1% and 1.6%, respectively (Figure 11). From these results it was found that, during June solstice, NN model performed well in estimating GPS TECv than the IRI model.

For the case of September solstice (Figure 9, left lower panel), NN model was again observed to well estimate the GPS TECv compared to IRI model. The correlation coefficients between GPS TECv and NN model and IRI model were equal to 0.9611 and 0.7854, respectively (Table 3). From Figure 10 it was observed that, the maximum and minimum errors of the NN model TECv from GPS TECv were respectively 8 TECU occurred at 21:00 UT and 0.02 TECU occurred at 4:00 TECU. From the same figure, it was further noted that, the maximum error of IRI model from GPS TECv was approximately 12.5 TECU occurred at 12:00 UT, while the minimum was about 0.4 TECU occurred at 7:00 UT. Correspondingly, the maximum relative error of the NN model to the GPS TECv was roughly 28%, and that of the IRI model was 42% (Figure 11). On the other hand, the minimum relative errors of NN model and IRI model to the GPS TECv were observed to be approximately 0.07% and 1.4%, respectively. Based on this information, it is concluded that, NN model estimated GPS TECv very well compared to IRI model, and that, IRI model performed better only during night times.

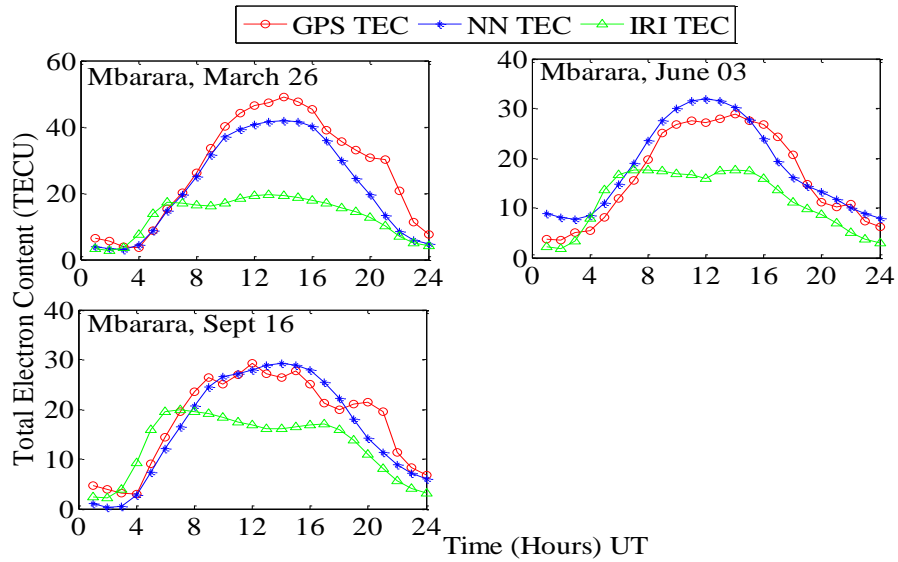


Figure 9: Seasonal comparison of GPS TECv with the corresponding predictions from NN model TECv and IRI-Neq model TECv at Mbarara for 2016.

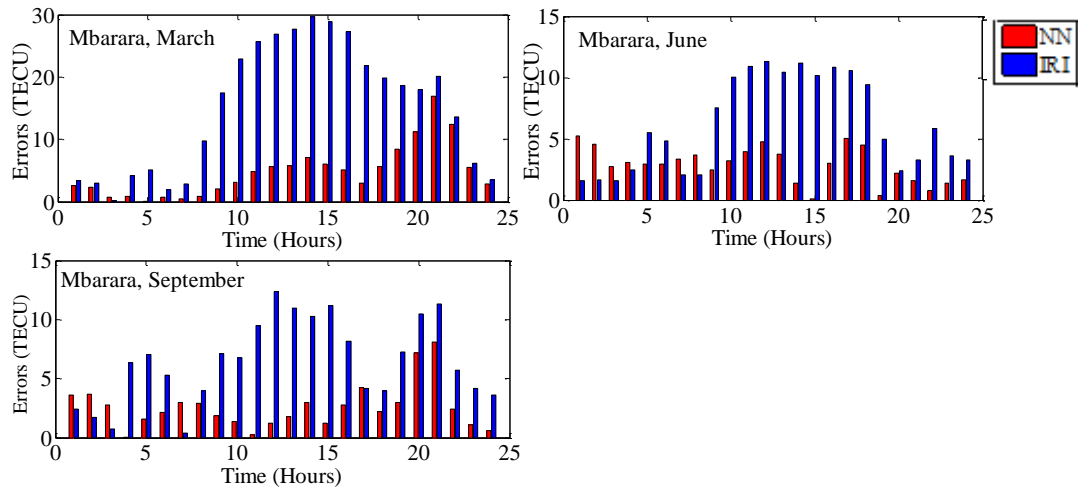


Figure 10: Errors of NN TECv and IRI TECv from GPS TECv for seasonal comparison at Mbarara for 2016.

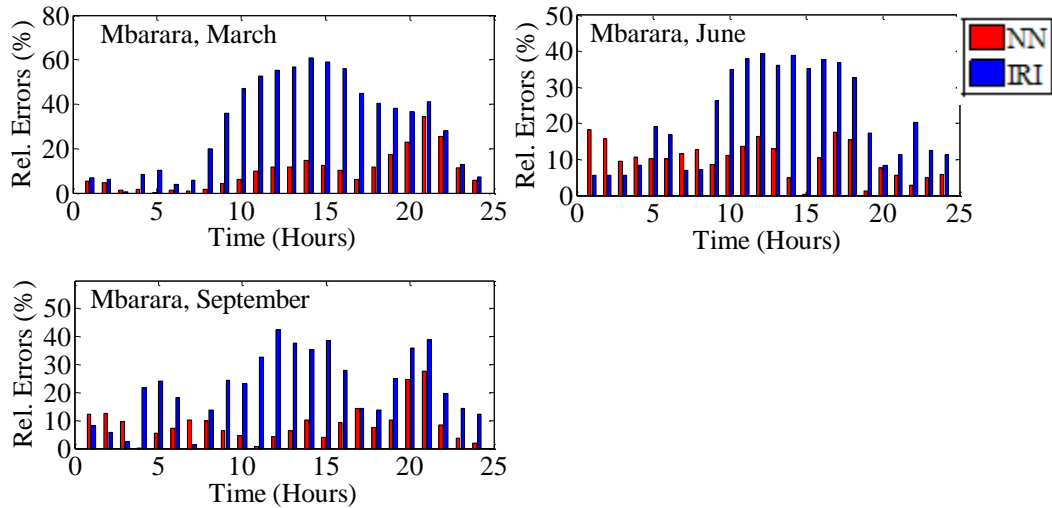


Figure 11: Relative errors of NN TECv and IRI TECv to GPS TECv for seasonal comparison at Mbarara for 2016.

Table 3: Seasonal correlation coefficients (r) for Mbarara (2016)

Model	March	June	September
NN	0.9647	0.9556	0.9611
IRI	0.8361	0.8428	0.7854

Despite good prediction of GPS TECv by the developed NN model, there were certain difficulties observed in predicting the GPS derived TECv during some periods. This might have been contributed by the fact that, this study was carried out during high solar activity where more TEC variations are evident. This is in agreement with the results obtained by Leandro and Santos (2007) in Brazil, Watthanasangmechai et al. (2012) in Thailand and Homam (2014) in Malaysia where the poorest absolute errors were attained during the period of high solar activity. Another reason for inaccuracy of NN model in predicting GPS TECv is the number of data set used in training. In NN modeling, an accuracy in predicting measured TECv is essentially contributed by a large data set for the training procedure (McKinnell and Poole 2004, Habarulema et al. 2007, Uwamahoro and

Habarulema 2015). At least an 11-year dataset is required as the results of the solar cycle variations. Conversely, due to a short period of availability of data in the region, a relatively small dataset used in model development may be somewhat responsible for the NN model's inaccuracy.

The capability of NN to predict GPS derived TECv has been achieved by other researchers globally. The NN model developed by Watthanasangmechai et al. (2012) in the equatorial latitude station in Thailand was able to predict TECv quite well, although there was a significant difficulty for it to learn during the TECv prediction process due to large variations of TECv. They associated that difficulty by the occurrence of an equatorial plasma bubble and to day-to-day TECv variations that occur in the equatorial region. A study by Habarulema et al. (2007) showed that, the NN model was able to predict the TECv values diurnally and seasonally more accurately than the IRI- 2001 over South Africa, although in some cases the model over or underestimated the TECv. Another study by Habarulema et al. (2011) showed the capability of NN to predict GPS TECv more accurately than the IRI-2001

model. He attributed this result by a scarcity of ionospheric data in Southern Africa that were used in developing IRI model. The same study showed that, correlation coefficients between the NN model and GPS TEC_v were more reliable as compared to those from the IRI-2001 model over South Africa. The accuracy of the prediction by the NN model results is more evident when the verification dataset used is within the training dataset range (Habarulema et al. 2011). Okoh et al. (2016), when they were comparing TEC_v predictions from the NN model and those from the IRI model, observed better predictions by the developed NN model than the IRI model. However, the results presented in this study do not challenge the strength and the effectiveness of global models like the IRI, but somewhat show that these models could assist as reliable supports when developing better regional models.

Conclusions

The NN architecture established comprised of seven input neurons; year, day of the year, hour of the day, geographic latitudes, geographic longitudes, SSN and IRI-NmF2. After training procedures, one hidden layer with 18 neurons was chosen as the one that provided the best results in this model. Moreover, the output of the NN used consisted of one neuron, which was the hourly TEC_v. The results showed that, the more input layer neurons were additionally included to the networks, the better the networks learned and gave the best results. Thus network 4 gave the optimal results since its RMSEs were lower than those from the other three networks, indicating good agreements between the measured values and the network predicted values when the NmF2 was added as an input neuron. It was also observed that, correlation coefficients indicated good levels of reliability of the developed NN model to predict GPS TEC_v when the IRI-NmF2 was included as an input neuron. This showed that the diurnal variational pattern of the TEC_v parameter was precise as predicted by the developed NN model. In addition to that, NN model was observed to closely match

the GPS TEC_v in most of the time compared to IRI-2012 model with NeQuick topside Ne option.

Acknowledgements

The authors wish to express the gratitude to the University Navstar Consortium (UNAVCO) for giving access to GPS data. The authors also acknowledge Dr. Gopi Seemala for providing access to the GPS-TEC analysis software used in this work.

References

- Bhuyan PK and Borah RR 2007 TEC derived from GPS network in India and comparison with the IRI. *Adv. Space Res.* 39(5): 830-840.
- Conway AJ, Macpherson KP, Blacklaw G and Brown JC 1998 A neural network prediction of solar cycle 23. *J. Geophys. Res.* 103: 29733-29742.
- Demuth H and Beale M 2002 Neural Network Toolbox for Use with MATLAB. User's Guide Version 4. The MathWorks, Inc. Natick, USA.
- Habarulema JB, McKinnell LA, and Cilliers PJ 2007 Prediction of global positioning system total electron content using Neural Networks over South Africa. *J. Atm. Solar-Terr. Phys.* 69(15): 1842-1850.
- Habarulema JB 2010 *A contribution to TEC modeling over Southern Africa using GPS data*. PhD Thesis, University of Rhodes.
- Habarulema JB, McKinnell LA, and Opperman BDL 2011 Regional GPS TEC modeling; attempted spatial and temporal extrapolation of TEC using neural networks. *J. Geoph. Res. Space Physics* 116: A04314.
- Homam MJ 2014 Initial Prediction of Total Electron Content (TEC) at a Low Latitude Station Using Neural Network. *2014 IEEE Asia-Pacific Conference on Applied Electromagnetics, 8-10 December, 2014 at Johor Bahru, Malaysia* 111-114.
- Jin H and Maruyama T 2009 3-3-2 Different behaviors of TEC and NmF2 observed during large geomagnetic storms. *J.*

- National Inst. Info. Comm. Technol.* 56(1-4): 369-376.
- Leandro RF and Santos MC 2007 A neural network approach for regional vertical total electron content modelling. *Stud. Geophys. Geodaet.* 51: 279-292.
- Leitinger R, Ciraolo L, Kersley L, Kouris SS and Spalla P 2004 Relations between electron content and peak density: Regular and extreme behaviour. *Annals of Geophysics* 47(2-3 SUPPL.): 1093-1107.
- Liu G, Huang W, Gong J and Shen H 2013 Seasonal variability of GPS-VTEC and model during low solar activity period (2006-2007) near the equatorial ionization anomaly crest location in Chinese zone. *Adv. Space Res.* 51(3): 366-376.
- McKinnell LA and Poole AWV 2004 Neural network-based ionospheric modelling over the South African region. *South Afr. J. Sci.* 100(11-12): 519-523.
- Norsuzila Y, Abdullah M, Ismail M, Ibrahim M and Zakaria Z 2010 Total Electron Content (TEC) and estimation of positioning error using Malaysia data. *World Congress on Engineering* 2010. 1: 715-719.
- Okoh D, Owolabi O, Ekechukwu C, Folarin O, Arhiwo G, Agbo J, Bolaji S and Rabiou B 2016 A regional GNSS-VTEC model over Nigeria using neural networks: A novel approach. *Geod. Geodynam.* 7(1): 19-31.
- Razin MRG, Voosoghi B and Mohammadzadeh A 2015 Efficiency of artificial neural networks in map of total electron content over Iran. *Acta Geodaet. Geophys.* 51(3): 541-555.
- Tulunay E, Senalp ET, Cander LR, Tulunay YK, Bilge AH, Mizrahi E, Kouris SS and Jakowski N 2004 Development of algorithms and software for forecasting, nowcasting and variability of TEC. *Ann. Geophys.* 47(2/3 SUPPL.): 1201-1214.
- Uwamahoro JC and Habarulema JB 2015 Modelling total electron content during geomagnetic storm conditions using empirical orthogonal functions and neural networks: *J. Geophys. Res. Space Phys.* 120: 11000-11012.
- Wattanasangmechai 2012 TEC prediction with neural network for equatorial latitude station in Thailand. *Earth, Planets Space* 64: 473-483.